Arch. Mech., 48, 6, pp. 1025–1045, Warszawa 1996

Experimental study of pseudoelastic behaviour of a Cu Zn Al polycrystalline shape memory alloy under tension-torsion proportional and non-proportional loading tests

C. ROGUEDA, C. LEXCELLENT and L. BOCHER (BESANÇON)

SOME TENSION-TORSION loading experiments on thin-walled tubular specimens of a Cu Zn Al polycrystalline shape memory alloy have been performed using a special experimental device. Proportional loading tests allow to verify the normality rule for the pseudoelastic strain rate and enable the experimental validation of the thermodynamical model of pseudoelastic behaviour developed by Raniecki *et al.* Non-proportional loadings show how the pseudoelastic behaviour depends on the chosen loading path. The chosen training path seems to have small effect on the obtained efficiency values which are very high (around 70 – 80 %). A microstructural experimental study must be done to understand the mechanism of formation and reorientation of martensite plates when the stress vector direction changes.

1. Introduction

THE MECHANICAL BEHAVIOUR of shape memory alloys (S.M.A.) is studied, as a rule, through some uniaxial tensile or compressive tests. As a consequence, mechanical models of, e.g., pseudoelastic behaviour, are usually written and also validated only in the case of uniaxial stress. However, it is necessary to understand the S.M.A. behaviour under multiaxial loading since it is the case in most of the industrial constructions. Some tests on mechanical structures have been performed for "complex" loadings: thin rectangular plates loaded in torsion [1], thin rectangular plates loaded in bending by a terminal force [2], springs loaded in tension [2] or in compression [3], ... But these tests were done either in order to study the efficiency of training, or in order to analyse the microstructure evolution.

In [4], B. RANIECKI *et al.* proposed a three-dimensional model of the pseudoelastic behaviour of S.M.A. In order to verify some of those hypotheses, the three-dimensional (3D), or at least two-dimensional (2D) loading tests have to be performed. The simplest two-dimensional loading to apply is a tension-torsion one. Some such experiments on SMA have been reported in [5] but the specimens used were rigid bar specimens (Cu Al Zn Mn) which were associated with an important shear stress gradient in torsion.

Some results of this kind of test on thin tubes are also reported in [6], but these experiments were performed on a Ni Ti polycrystal and the results are still quite qualitative. Moreover, only a few tests were performed.

In this paper, the experimental device and the results of proportional loading tests are discussed. Some non-proportional loading tests are also exposed, to show the importance of the loading sequence. Training of samples during these tests

http://rcin.org.pl

have been analyzed. Finally, the modelling described in [4] (and applied to proportional loading tests) is used to show a reasonable agreement with experimental data.

2. Material and technique

The tests have been performed on a Cu Zn Al polycrystalline S.M.A. without any additional components (weight composition: Cu 70.17 %, Zn 25.63 %, Al 4.2 %) prepared by the "Tréfimétaux" company. Its characteristic phase transformation temperatures, determined by home electric measurements, are 287 K for M_S, 278 K for M_F (temperature start – and end – of the austenite to martensite phase transformation) and 290 K for A_S, 293 K for A_F (temperature start – and end – of the reverse transformation). The heat treatment is quite standard. Specimens are heated at 1123 K during 15 minutes, quenched in a 393 K oil bath and maintained at this temperature for one hour. The specimens are carried out few days later, in order to make the austenitic phase more stable.

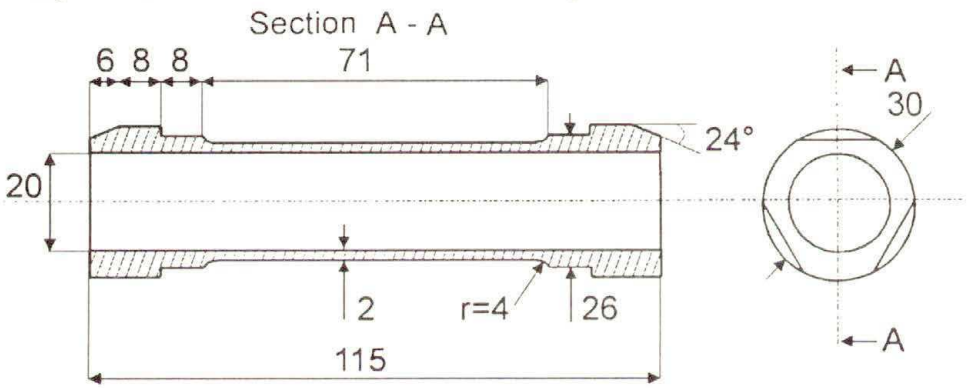

FIG. 1. Sample shape definition.

In order to avoid internal stresses, samples were manufactured by electro-erosion technique from 30 mm diameter rigid bars. Their dimensions (given in Fig. 1) are characteristic for thin tubes condition. During the tension-torsion tests, the stress tensor has the form:

$$\boldsymbol{\sigma} = \begin{pmatrix} 0 & 0 & 0 \\ 0 & 0 & \sigma_{z\theta} \\ 0 & \sigma_{z\theta} & \sigma_{zz} \end{pmatrix}, \tag{2.1}$$

with

$$\sigma_{zz} = F/2\pi Re, \qquad \sigma_{z\theta} = C/2\pi R^2 e, \tag{2.2}$$

F, C, R and e are, respectively, the axial loading force, the torque, the mean radius and thickness of the sample. It must be remembered that in the S.M.A.

http://rcin.org.pl

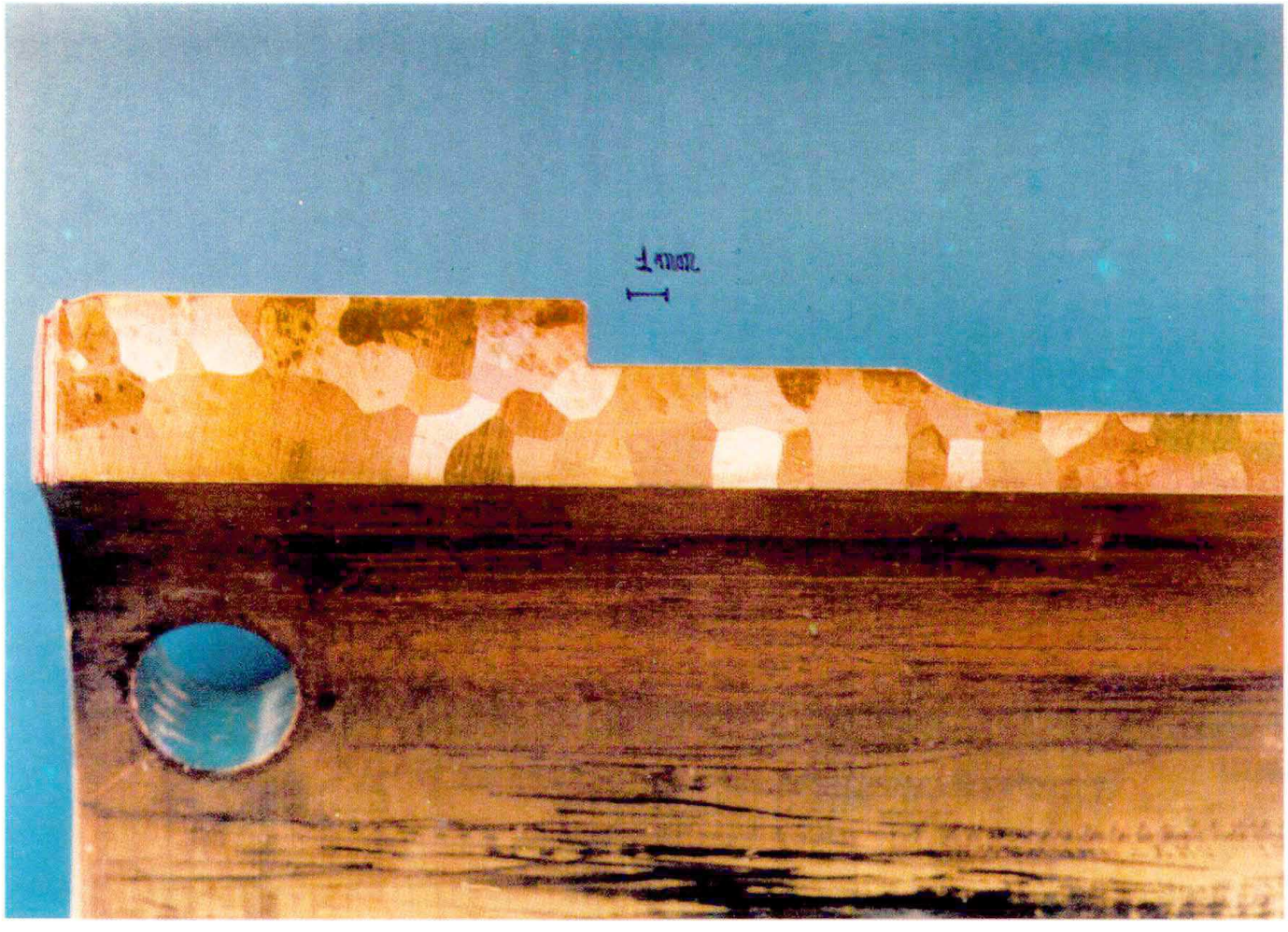

FIG. 2. Photograph of the sample.

http://rcin.org.pl

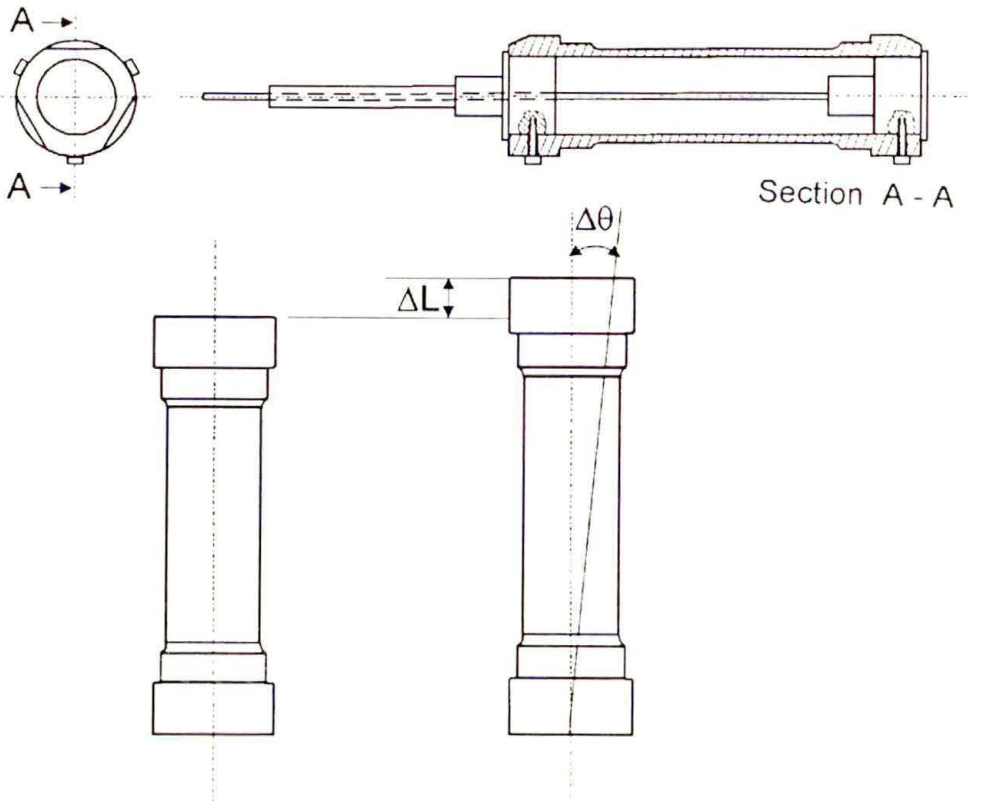

FIG. 3. Strain measurement device.

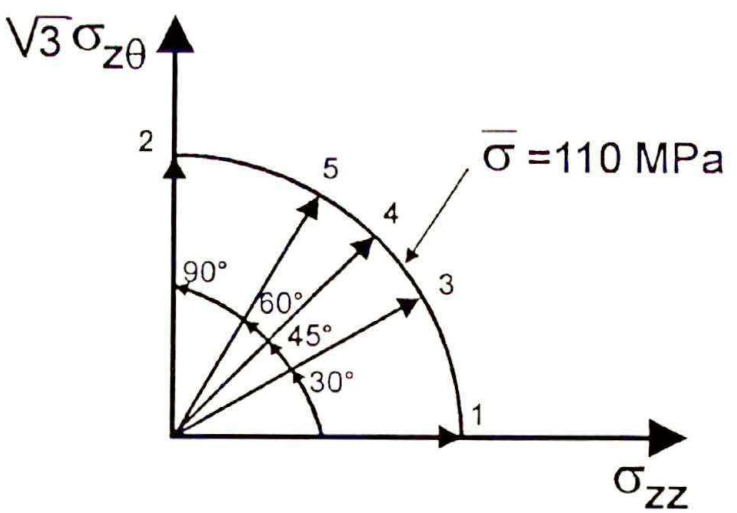

FIG. 4. Repartition of the five proportional loading tests on $\overline{\sigma}_{max}$ = 110 MPa.

http://rcin.org.pl

case, the thin tube condition must take into account the mean grain size which is about 1 mm (see Fig. 2). Some 1800 grains have been numbered in the measured part.

The sample shape is adapted to a specific mechanical device which takes over the whole loading and ensures the specimen to be properly fixed. Tests were performed on a Schenk 3D test machine (tension, torsion and internal pressure), connected with the H.P. microcomputer. This hydraulic machine has load limits ± 63 kN and ± 1000 Nm. Every test has been performed under a force control.

The temperature was maintained constant at $T = 303$ K ($T > A_F$).

Stresses are calculated from F and C values with the accuracy of ± 3.1 N and ± 0.12 Nm. Axial and torsional strains are obtained from a mechanical differential system illustrated in the Fig. 3. Linear and rotative sensors (L.V.D.T and R.V.D.T) are linked to each stem of this system, in order to separate strain components from each other. They measure axial and angular displacements (ΔL and $\Delta\theta$).

Assuming the strains to be small, axial and torsional strains ε_{zz} and $\varepsilon_{z\theta}$ can be easily calculated from the formulae

$$\varepsilon_{zz} = \Delta L / L, \qquad \varepsilon_{z\theta} = \frac{r\Delta\theta}{2L}. \tag{2.3}$$

Here L is the effective length, estimated by means of a classical extensometer to be equal 69 mm. Displacements are known with the accuracy of $\pm 5 \cdot 10^{-6}$ m for the axial sensor and $\pm 1.22 \cdot 10^{-3}$ rad. for the angular one.

Strain gauges were also tried but it was so difficult to obtain a good adherence between the sample and gauges that this technique has been abandoned. This behaviour is probably due to copper corrosion.

3. Experimental results

3.1. Proportional loading tests

In tension-torsion loading tests, the equivalent stress, in agreement with the von Mises criterion, is defined by

$$\overline{\sigma} = \left(\sigma_{zz}^2 + 3\sigma_{z\theta}^2\right)^{1/2}. \tag{3.1}$$

For each proportional test, the maximum equivalent stress $\overline{\sigma}_{\max}$ is 110 MPa. Hence, each point corresponding to the end of loading belongs to a quarter of circle, the radius of which is $\overline{\sigma}_{\max}$ in the $(\sigma_{zz}, \sqrt{3}\sigma_{z\theta})$-plane representation. The courses of the five tests performed in this quarter of circle is presented in the Fig. 4. As the loading is proportional, axial and torsional stresses are connected with each other by the relation

$$\sigma_{z\theta} = \alpha\sigma_{zz} \qquad (\alpha = C^{te}). \tag{3.2}$$

http://rcin.org.pl

The value of α, fixed in each test, characterizes the direction of loading and can vary between 0 (pure tensile test) and ∞ (pure torsional test).

The test frequency is 10^{-3} Hz. Loading and unloading periods are similar. The first cycle is repeated 35 times in order to evaluate the possible training of the samples.

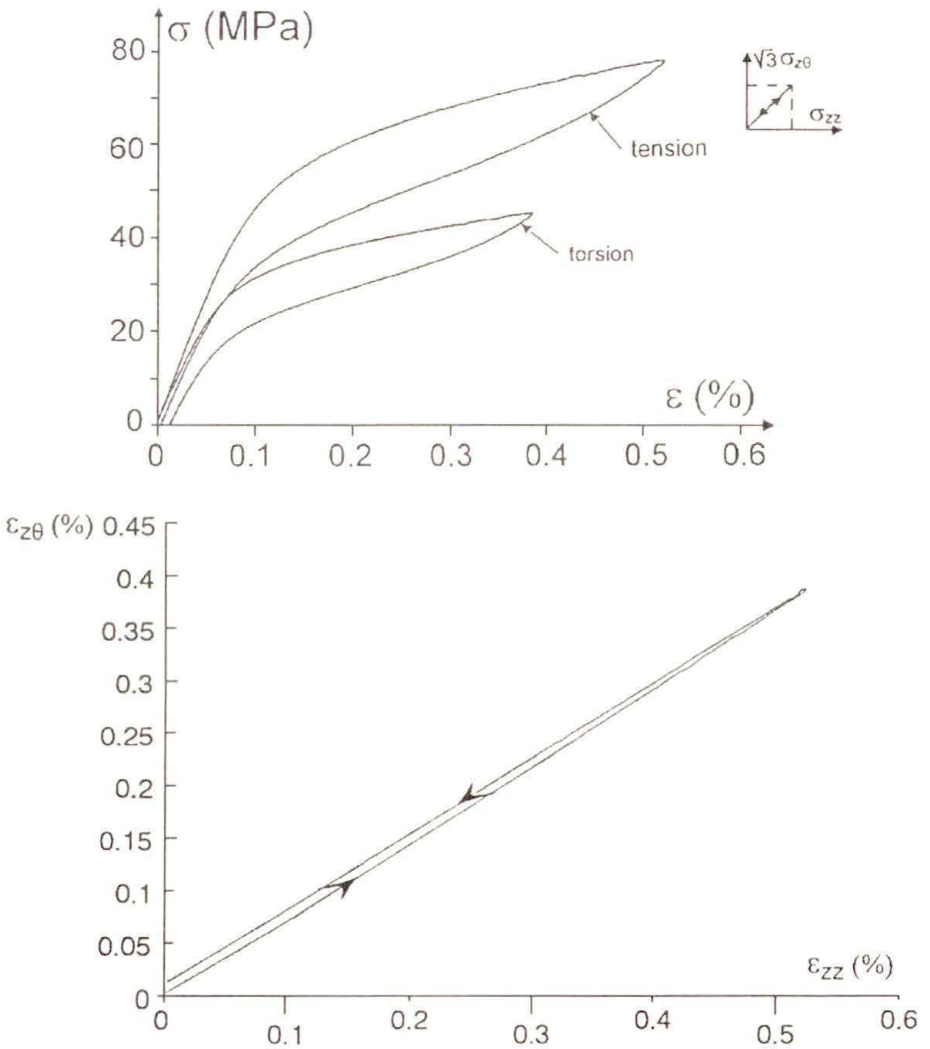

FIG. 5. Tension-torsion proportional loading test (α = 0.577).

The stress-strain curve corresponding to the No. 4 test (α = 0.577) is presented in Fig. 5, as a representative test. In the following parts of this paper, the elastic behaviour, the yield stress of phase transition, the pseudoelastic behaviour and finally the training efficiencies are studied.

http://rcin.org.pl

3.1.1. Classical elastic behaviour. Elastic strains and stresses are related by the Poisson coefficient ν and the Young modulus E as follows:

$$\begin{aligned} \varepsilon^e_{rr} &= \varepsilon^e_{\theta\theta} = -\frac{\nu}{E}\sigma_{zz}\,, & \varepsilon^e_{zz} &= \frac{1}{E}\sigma_{zz}\,, \\ \varepsilon^e_{z\theta} &= \frac{1+\nu}{E}\sigma_{z\theta}\,, & \varepsilon^e_{r\theta} &= \varepsilon^e_{rz} = 0. \end{aligned} \tag{3.3}$$

E and ν are calculated from the slope of each stress-strain curve. A considerable scatter of E values can be observed. This can be explained by a possible dispersion during heat treatment because the samples are thick, or by a relative non-homogeneity of the alloy. This observation in the elastic domain, where the behaviour is well known, is important to estimate the dispersion of further results.

3.1.2. Yield stress of phase transformation. To characterize the beginning of the direct phase transformation (i.e. austenite to martensite), the usual von Mises yield stress is defined as:

$$\overline{\sigma}^{AM} = \left((\sigma^{AM}_{zz})^2 + 3(\sigma^{AM}_{z\theta})^2\right)^{1/2}, \tag{3.4}$$

where (σ^{AM}_{zz}) and $(\sigma^{AM}_{z\theta})$ are the axial and torsional threshold stresses. They correspond to the linearity loss of the $(\varepsilon_{zz}, \sigma_{zz})$ and $(\varepsilon_{z\theta}, \sigma_{z\theta})$ curves. For each test, the $\overline{\sigma}^{AM}$ value is calculated and $\left((\sigma^{AM}_{zz}), \sqrt{3}(\sigma^{AM}_{z\theta})\right)$ are given on the $(\sigma_{zz}, \sqrt{3}\sigma_{z\theta})$ plane. As it is shown in Fig. 6, $\overline{\sigma}^{AM}$ seems to be rather constant in these tests, and a criterion surface can be defined as $\overline{\sigma}^{AM} = 30.3$ MPa.

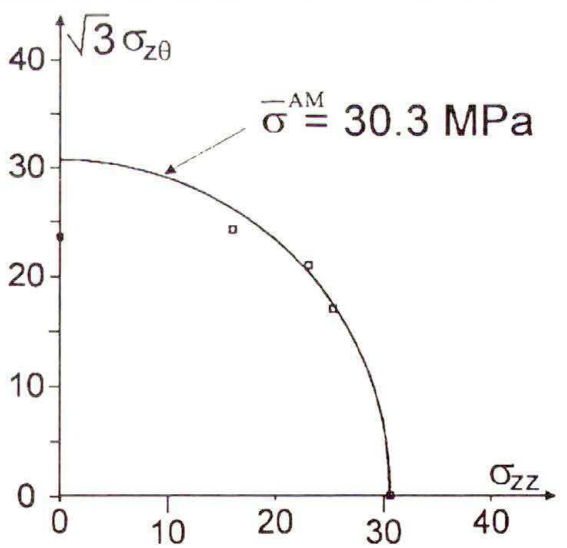

FIG. 6. Yield surface phase transformation: austenite → martensite.

http://rcin.org.pl

In a tensile test, the critical stress σ^{AM} and the temperature T are linked by the following relation:

$$\sigma^{AM} = b(T - M_S). \tag{3.5}$$

Generalizing this relation for multidimensional loading tests, the constant b is found to be equal to $1.9\,\mathrm{MPaK}^{-1}$ which is a known value for a Cu Zn Al polycrystal. In [7], uniaxial tests with the same alloy were presented and b was estimated to be $2.0\,\mathrm{MPaK}^{-1}$.

3.1.3. Study of pseudoelastic behaviour. First, the total deformation is split into two parts, the elastic and the pseudoelastic deformation:

$$\boldsymbol{\varepsilon} = \boldsymbol{\varepsilon}^e + \boldsymbol{\varepsilon}^{pe}. \tag{3.6}$$

For tensile tests, VACHER in [7] has established the proportionality between the pseudoelastic deformation and the volume fraction of martensite, by performing the electrical resistance measurements during mechanical tests.

For a 2D or a 3D proportional loading, as in "plasticity", the existence of a current flow surface ($\overline{\sigma}$ = cte) is postulated. It is homothetic to the initial one ($\overline{\sigma}^{AM}$ = cte); the normality rule, i.e. the pseudoelastic strain rate is perpendicular to this surface.

In a classical way, it follows that

$$\dot{\boldsymbol{\varepsilon}}^{pe} = \dot{\lambda}\frac{\partial f}{\partial \boldsymbol{\sigma}}, \tag{3.7}$$

with

$$f = \overline{\sigma} - \overline{\sigma}^{AM}(T), \qquad \dot{\lambda} = \gamma\dot{z}. \tag{3.8}$$

So, the pseudoelastic strain rate is obtained as

$$\dot{\boldsymbol{\varepsilon}}^{pe} = \frac{3}{2}\frac{\operatorname{dev}\boldsymbol{\sigma}}{\overline{\sigma}}\gamma\dot{z}, \tag{3.9}$$

where γ is the maximal pseudoelastic strain obtained for a complete phase transformation occurring in a tensile test.

In a tension-torsion proportional loading test, the expressions (3.2) and (3.9) lead to:

$$\begin{aligned}
\dot{\varepsilon}^{pe}_{zz} &= \frac{\sigma_{zz}}{\overline{\sigma}}\gamma\dot{z} = \frac{1}{(1+3\alpha^2)^{1/2}}\gamma\dot{z},\\
\dot{\varepsilon}^{pe}_{\theta\theta} &= \dot{\varepsilon}^{pe}_{rr} = -\frac{1}{2}\dot{\varepsilon}^{pe}_{zz},\\
\dot{\varepsilon}^{pe}_{z\theta} &= \frac{3}{2}\frac{\sigma_{z\theta}}{\overline{\sigma}}\gamma\dot{z} = \frac{3}{2}\frac{\alpha}{(1+3\alpha^2)^{1/2}}\gamma\dot{z}.
\end{aligned} \tag{3.10}$$

http://rcin.org.pl

In this case, the integration yields

$$\boldsymbol{\varepsilon}^{pe} = \frac{3}{2}\frac{\operatorname{dev}\boldsymbol{\sigma}}{\overline{\sigma}}\gamma z. \tag{3.11}$$

It is possible to evaluate $\varepsilon^{pe}_{\theta\theta}/\varepsilon^{pe}_{zz}$ from strain measurements obtained by the gauges. As it is shown in Fig. 7, the experimental value of $\varepsilon^{pe}_{\theta\theta}/\varepsilon^{pe}_{zz}$ is not far from the theoretical value which is -0.5. The small dispersion can result from the position of the gauges.

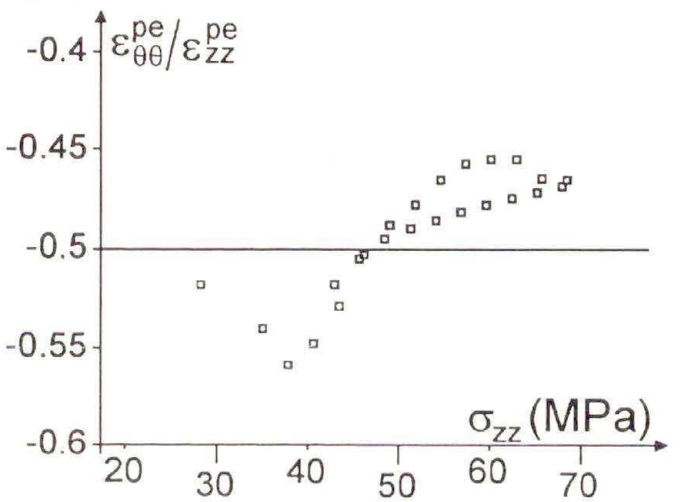

FIG. 7. Ratio $\varepsilon^{pe}_{\theta\theta}/\varepsilon^{pe}_{zz}$ evolution during a tensile-torsion proportional loading.

Validity of the expression (3.11) is verified by studying the evolution of $\varepsilon^{pe}_{z\theta}/\varepsilon^{pe}_{zz}$. Parameter Q is defined as:

$$Q = \frac{\varepsilon^{pe}_{zz}}{\varepsilon^{pe}_{z\theta}}\frac{\sigma_{z\theta}}{\sigma_{zz}}. \tag{3.12}$$

From (3.11) it follows that Q is theoretically constant and equal to 2/3. The evolution of Q with respect to the tensile stress σ_{zz} during the test No. 4 ($\alpha = 0.577$) is presented in the Fig. 8. It can be noticed that even though Q seems to be a constant, its value is slighty higher than the theoretical one. Q values for the three biaxial loading tests are presented in the Tab. 1.

Table 1. Value of Q obtained for each proportional test.

Test	3	4	5
Q	0.72	0.75	0.75

http://rcin.org.pl

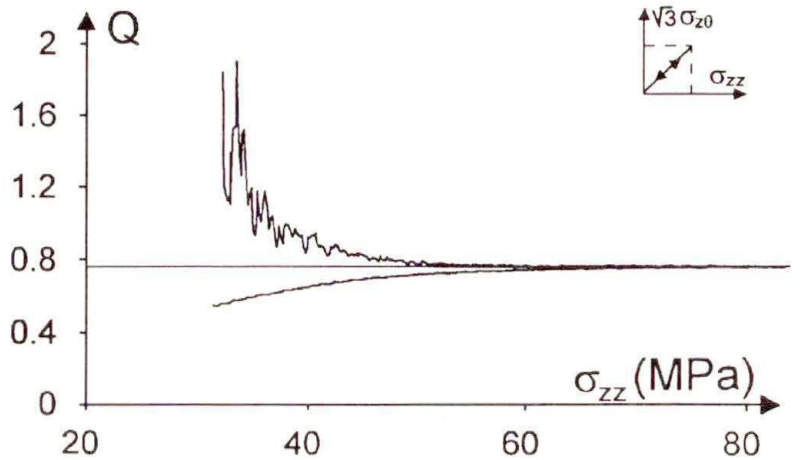

FIG. 8. Experimental evolution of the Q parameter (during the test described in Fig. 5).

The equivalent pseudoelastic strain is defined by:

$$\overline{\varepsilon}^{pe} = \left[(\varepsilon_{zz}^{pe})^2 + \frac{4}{3} (\varepsilon_{z\theta}^{pe})^2 \right]^{1/2}. \tag{3.13}$$

Its maximum value is reached when $\overline{\sigma}$ is maximum ($\overline{\sigma}_{\max} = 110\,\mathrm{MPa}$). The Tab. 2 shows $\overline{\varepsilon}_{\max}^{pe}$ for each test. In a pure tension test, $\varepsilon_{z\theta}^{pe}$ is theoretically null, and in a pure torsional test, ε_{zz}^{pe} is also zero. From the Tab. 2, the material seems to be slightly anisotropic. This can explain why Q is not equal to its theoretical value.

Table 2. Experimental tensile and torsional pseudoelastic strain values.

Test	1	2	3	4	5
ε_{zz}^{PE} (%)	0.339	0.011	0.384	0.369	0.193
$\varepsilon_{z\theta}^{PE}$ (%)	0.025	0.215	0.173	0.277	0.356
$\overline{\varepsilon}^{PE}$ (%)	0.34	0.248	0.433	0.488	0.454

The pseudoelastic strain measurements allow also to determine the pseudoelastic strain rate vector $\dot{\boldsymbol{\varepsilon}}^{pe}$. As the loading is proportional, the following relation holds (expressions (3.9) and (3.11)):

$$\frac{\varepsilon_{z\theta}^{pe}}{\varepsilon_{zz}^{pe}} = \frac{\dot{\varepsilon}_{z\theta}^{pe}}{\dot{\varepsilon}_{zz}^{pe}}. \tag{3.14}$$

Then, it is easy to draw $\dot{\boldsymbol{\varepsilon}}^{pe}$ on the $(\sigma_{zz}, \sqrt{3}\sigma_{z\theta})$ plane, for each test, when the equivalent stress is maximal, as it is shown in the Fig. 9. This figure shows also that

http://rcin.org.pl

the strain rate vector is perpendicular to the loading surface ($\overline{\sigma}_{\max} = 110\,\text{MPa}$) what proves the validity of the normality rule. Moreover, it allows to see the expansion of the criterion surface from $\overline{\sigma}^{AM} = 30.3\,\text{MPa}$ to $\overline{\sigma}_{\max} = 110\,\text{MPa}$.

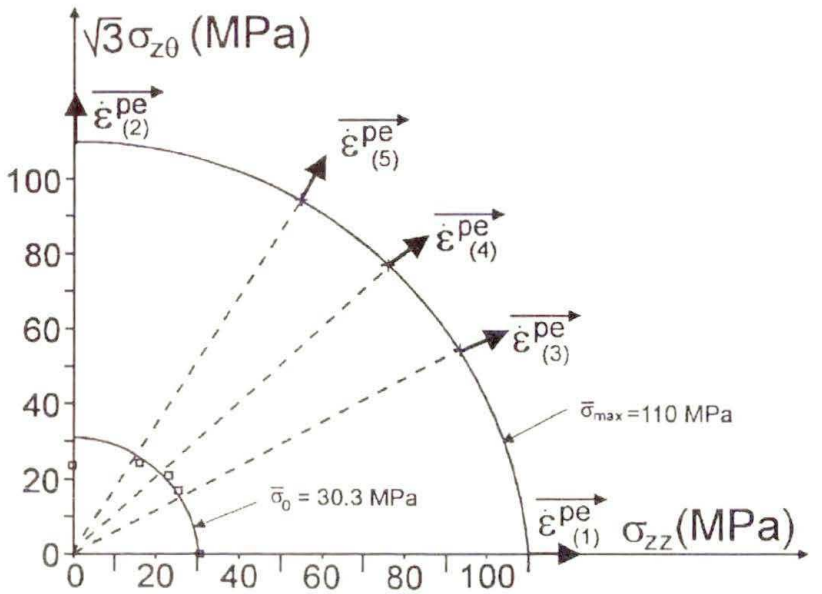

FIG. 9. Experimental validation of the normality rule.

3.1.4. The training process. After $N_{\max} = 35$ loading-unloading cycles (between $\overline{\sigma} = 0$ and $\overline{\sigma} = \overline{\sigma}_{\max} = 110\,\text{MPa}$), the training effect is measured. Figure 10 represents the first ten cycles corresponding to the test No. 4. The Fig. 11 shows the training effect in this sample, placed (at a stress-free state) in an oil bath of temperature varying from 232 K to 313 K.

In order to study the training effect, it is necessary to define three training efficiencies: the tension efficiency ($\varrho_{zz} = (\Delta\varepsilon_{zz})_{\sigma=0}/(\varepsilon^{pe}_{zz\,\max})_{N=N_{\max}}$), the torsion efficiency ($\varrho_{z\theta} = (\Delta\varepsilon_{z\theta})_{\sigma=0}/(\varepsilon^{pe}_{z\theta\,\max})_{N=N_{\max}}$) and the equivalent efficiency ($\varrho = (\Delta\overline{\varepsilon})_{\sigma=0}/(\overline{\varepsilon}^{pe}_{\max})_{N=N_{\max}}$).

These efficiencies are measured for the five training tests. These values seem to be much higher (around 75–80%) than the ones obtained under a more complex loading (c.f. for example [1]). In [5], where rigid bars are also loaded in tension and torsion, the first cycle is repeated in order to study the stabilization of stress-induced martensite. Unfortunately, the efficiency values are not presented. Nevertheless, the pseudoelastic loop stabilizes after a few cycles, as in our experiments. Training values lead us to assume that the density of dislocations is quite important since, according to [8], the density of dislocations is a good parameter helping to evaluate the training effect. Until now, no microstructural analysis has been performed to verify the assumption.

http://rcin.org.pl

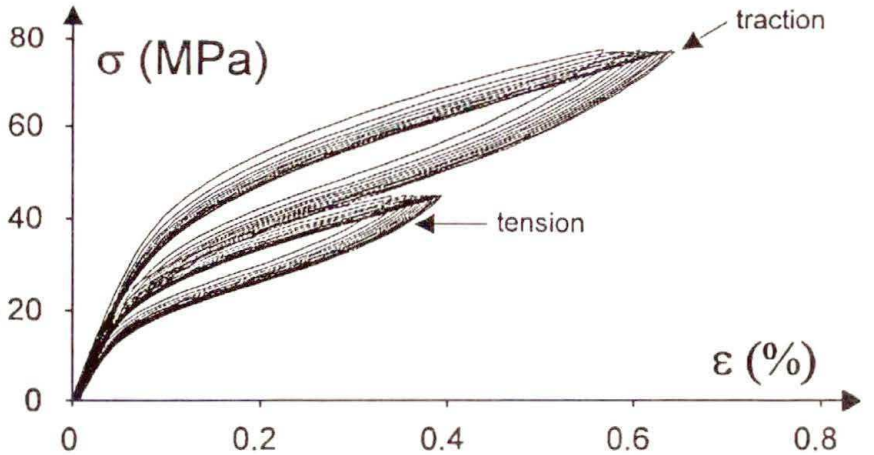

FIG. 10. The first ten half-cycles of a training process (test No. 4, $\alpha = 0.577$).

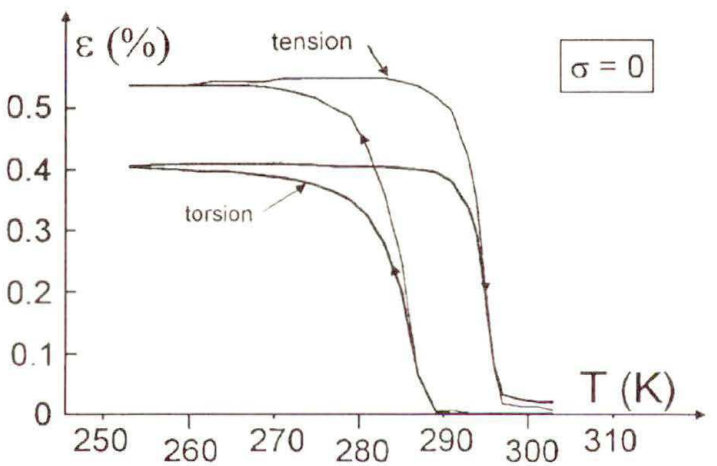

FIG. 11. Two-way shape memory effect measured after training process of Fig. 10.

3.2. Non-proportional tests

Even if the modelling of non-proportional loadings is, in most of cases, not simple, the importance of such tests appears to be in answering the queston: "what is the effect of a rough change of the mechanical loading upon the material behaviour?" Indeed, in every single crystal, the best oriented habit planes are activated (with respect to the maximum shear rule) for a given loading direcion [9]. If the direction of the stress vector is changed by applying torsion upon the tension, other variants ("secondary variants") can be activated and interact vith the primary variants. Here, it is interesting to see what happens macroscopically to a polycrystalline sample.

http://rcin.org.pl

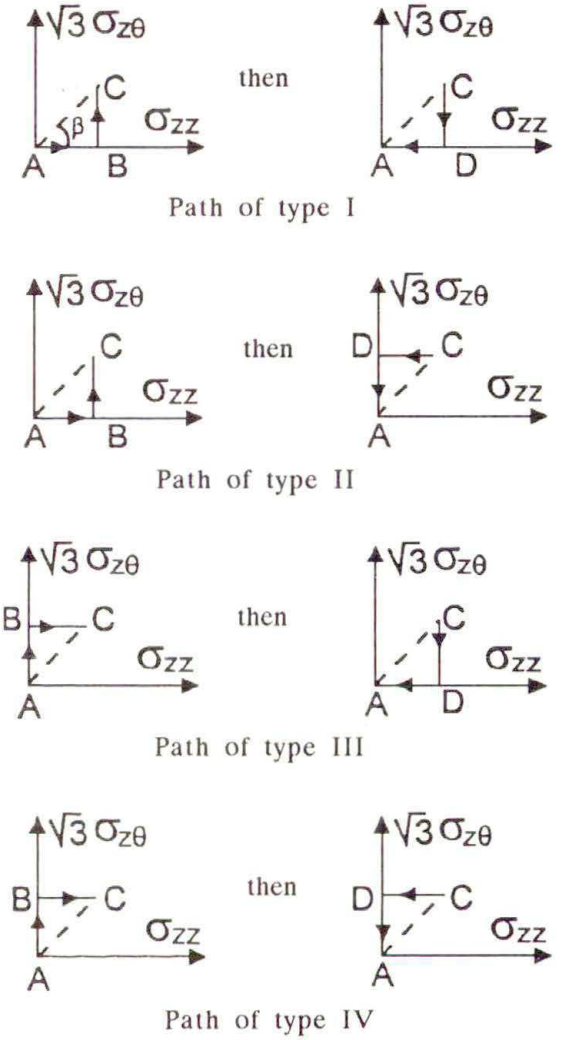

FIG. 12. Definition of non-proportional paths.

As in the proportional loading tests, the maximum equivalent stress $\overline{\sigma}_{\max}$ is 110 MPa, but it is reached through four different possible paths: I, II, III and IV (see Fig. 12). β is the angle characterizing the test $[\mathrm{tg}\,\beta = (\sqrt{3}\,\sigma_{z\theta}^{\max})/\sigma_{zz}^{\max}]$. Its possible values are 30°, 45°, 60° as in the respective tests 3, 4 and 5 with proportional loading.

3.2.1. Pseudoelastic loop of the first cycle. For each path, the tensile $(\sigma_{zz}, \varepsilon_{zz})$ and torsional curves $(\sigma_{z\theta}, \varepsilon_{z\theta})$ are given (Figs. 13 to 16). So, the resulting deformation path $(\varepsilon_{z\theta}, \varepsilon_{zz})$ is known. As it was already observed in the previous part, material

http://rcin.org.pl

isotropy is not perfect since during the first loading (uniaxial), the small strain is measured along the other axis.

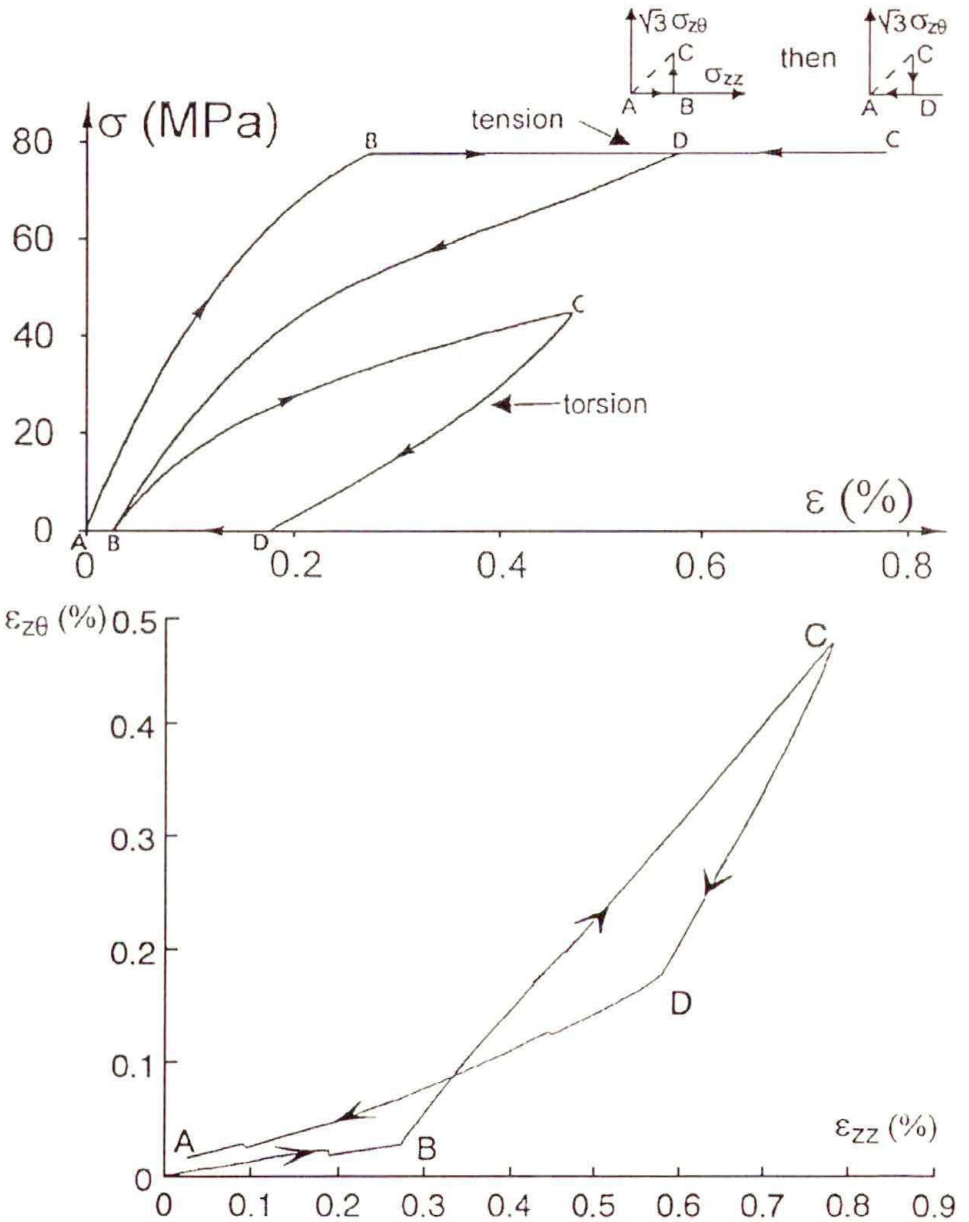

FIG. 13. Tension-torsion non-proportional loading test (path I, $\beta = 45°$).

Maximum equivalent pseudoelastic strain $\bar{\varepsilon}^{pe}_{max}$ is higher than that in the proportional loading tests. This observation confirms the assumption that new habit planes ("secondary" planes) are activated when the mechanical loading direction

http://rcin.org.pl

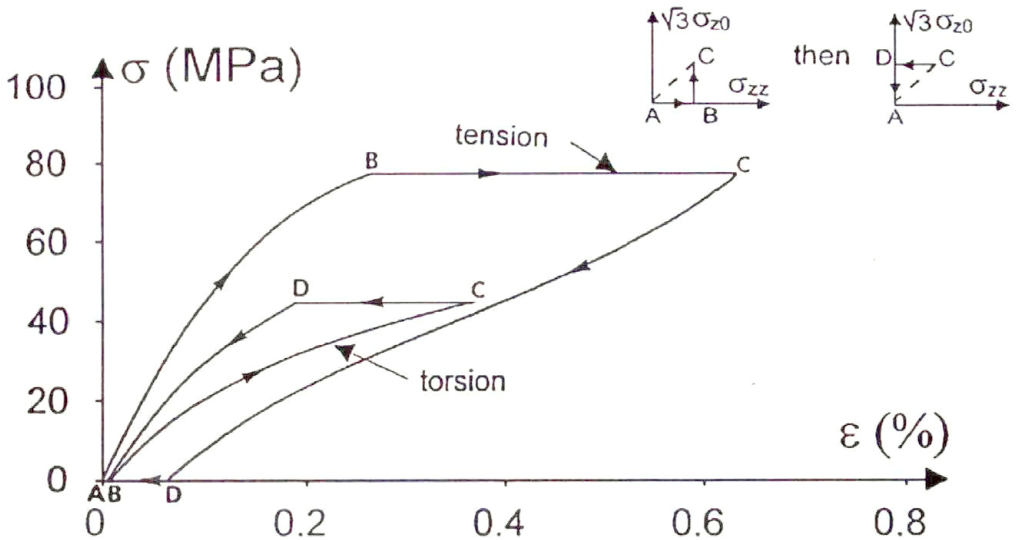

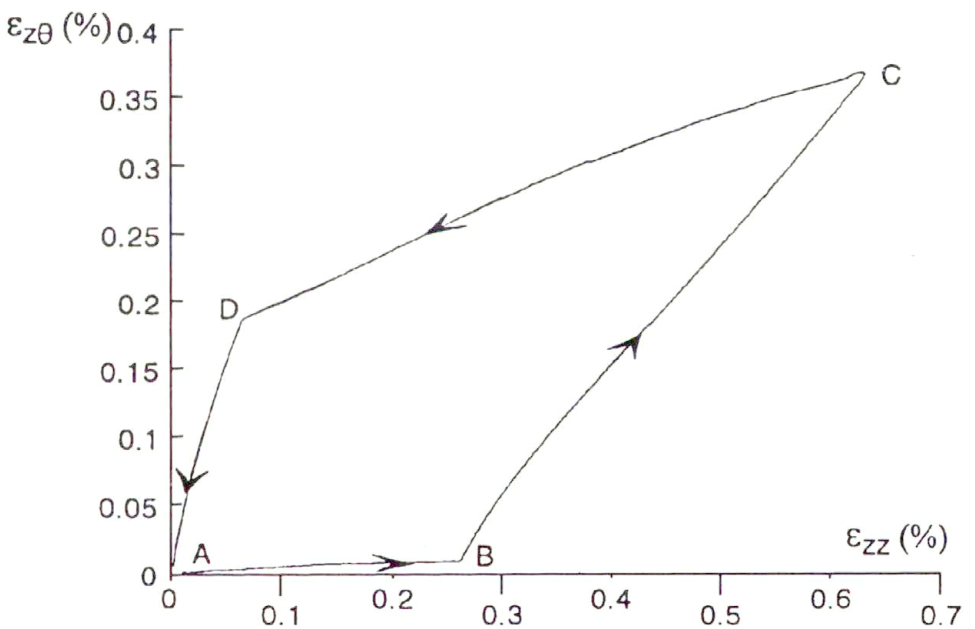

FIG. 14. Tension-torsion non-proportional loading test (path II, $\beta = 45°$).

changes. Moreover, it seems that the hardening induced by interactions between primary and secondary habit planes does not play any important role. Moreover, during the second loading (BC), a reorientation of primary variants may occur with the change of the stress vector orientation. Such variant reorientations are reported in [5].

http://rcin.org.pl

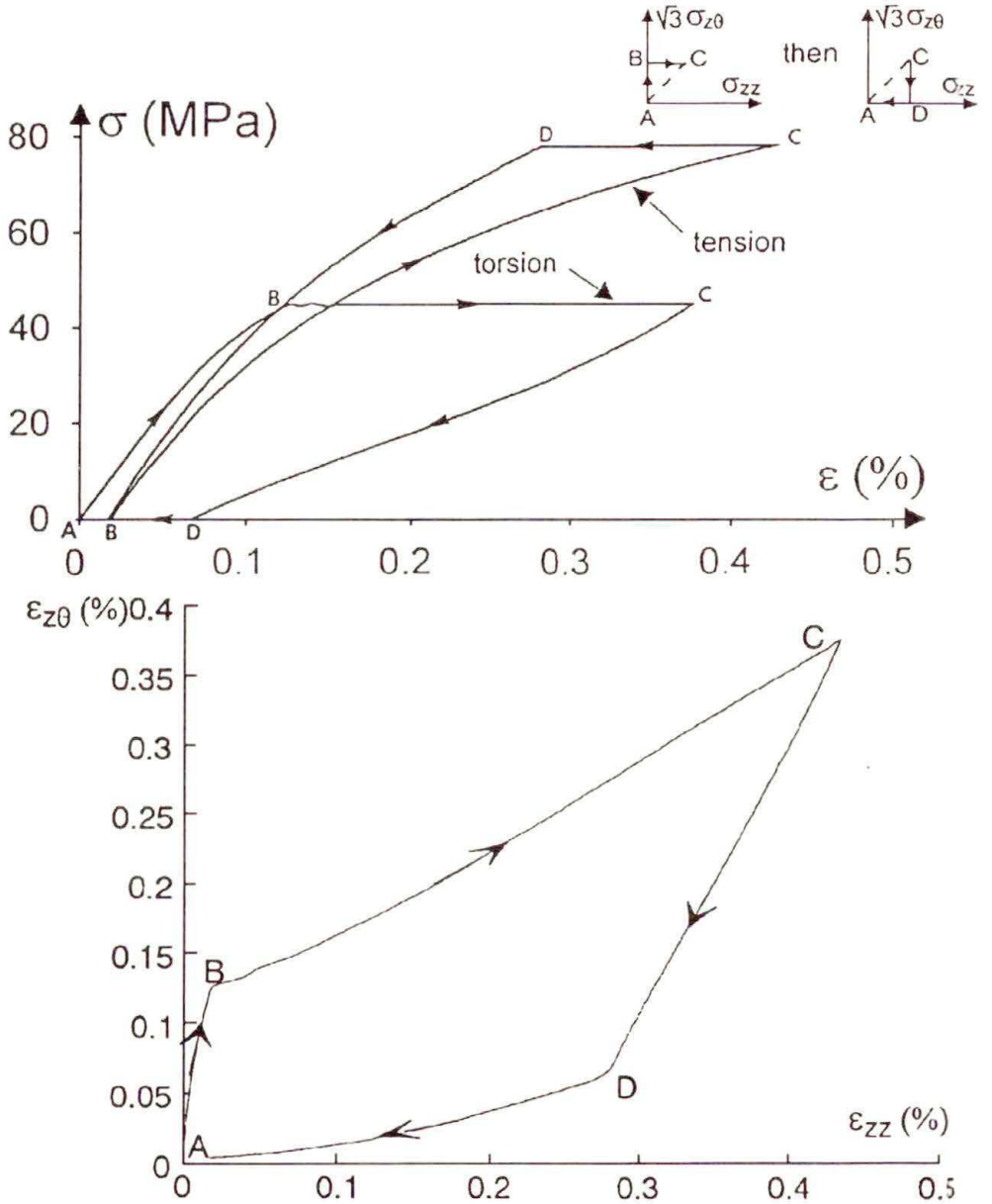

FIG. 15. Tension-torsion non-proportional loading test (path III, $\beta = 45°$).

In fact, during these non-proportional loading tests, observation of the microstructure evolution is necessary to understand the micromechanisms invoved by the stress path. From the phenomenological point of view, the comparson between the shape of the imposed stress path (rectangular in Figs. 14 and 15) and the resulting shape in the deformation path is interesting.

http://rcin.org.pl

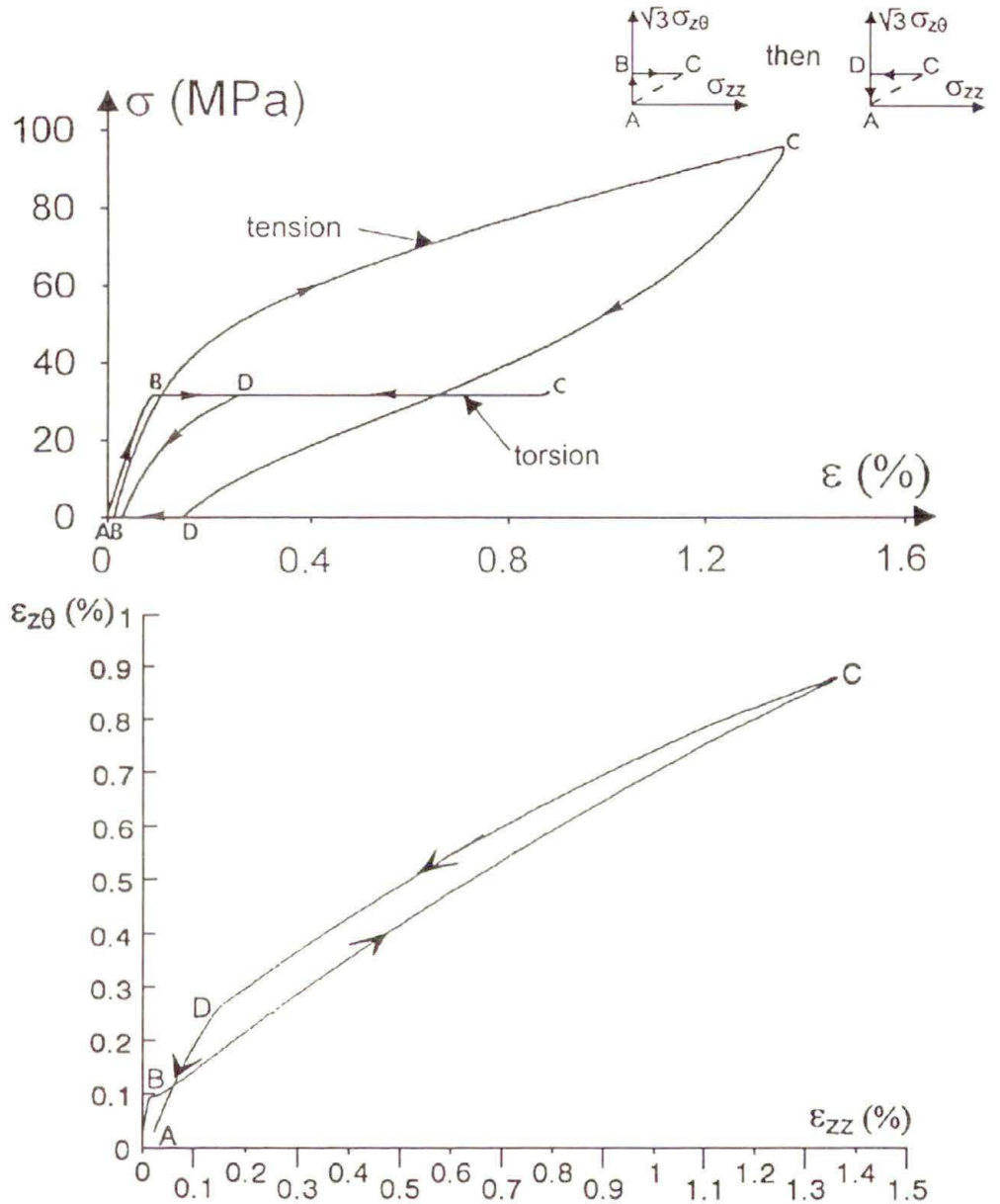

FIG. 16. Tension-torsion non-proportional loading test (path IV, $\beta = 30°$).

3.2.2. The training process. The ten first cycles of a training are presented in Fig. 17. After $N = N_{max} = 35$ cycles, the training effect is measured (Fig. 18). Efficiency definitions are the same as in the previous case.

The global efficiency ϱ lies between 60 and 80 % and its dependence on the chosen path is not clear.

http://rcin.org.pl

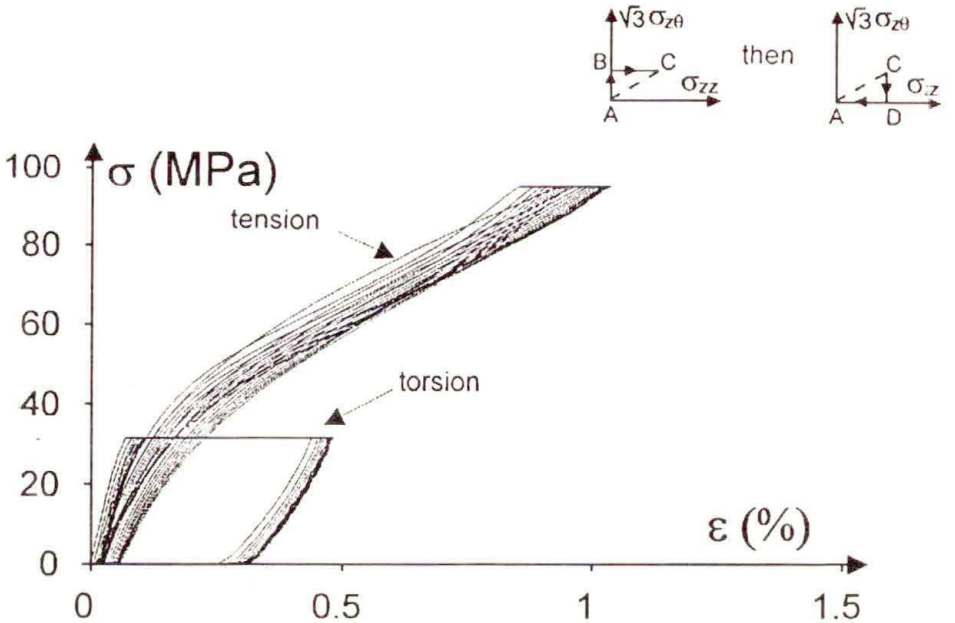

FIG. 17. The first ten half-cycles of a non-proportional loading training process (path III, $\beta = 30°$).

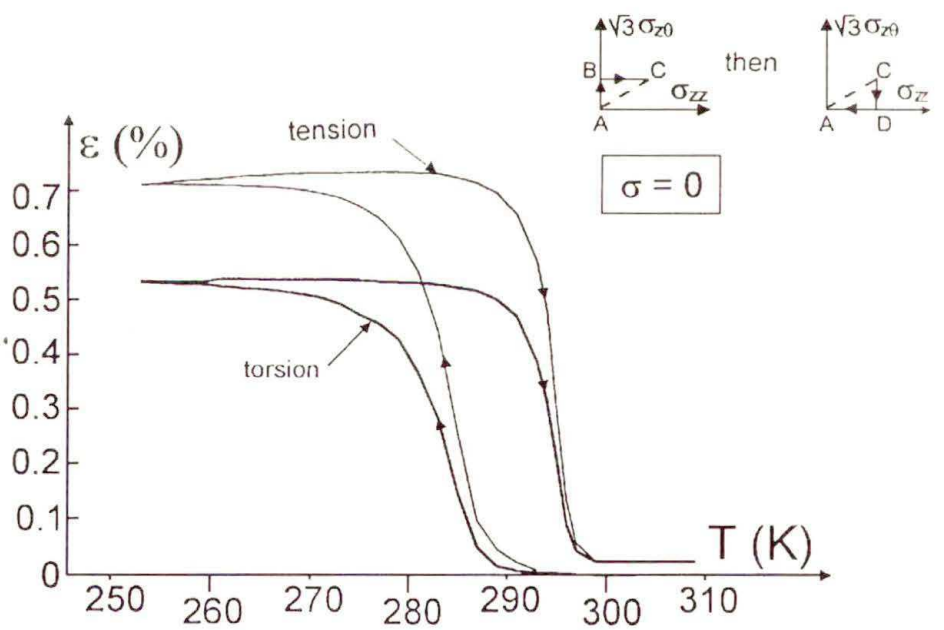

FIG. 18. Two-way shape memory effect measured after training process of Fig. 17.

http://rcin.org.pl

4. Modelling of a proportional loading test

4.1. General equations

In [4], RANIECKI *et al.* propose to model the pseudoelastic behaviour in two steps. First, the free energy of the two phases system $(A + M)$ is written as

$$\Phi = (1 - z)\Phi_1 + z\Phi_2 + \Delta\Phi. \tag{4.1}$$

Φ_1 and Φ_2 are the specific free energies of the austenite and of the martensite phases, respectively. $\Delta\Phi$ is called the configurational energy and represents the interaction which appears between the two phases, for example produced by incompatibilities between deformations. The main property of this energy is that it disappears if only one phase is present in the material. In agreement with MULLER and XU [10], the simplest expression for $\Delta\Phi$ is:

$$\Delta\Phi = z(1 - z)\Phi_{it}\,, \tag{4.2}$$

where Φ_{it} is the interaction energy $(\Phi_{it}(T) = \overline{u}_0 - T\overline{s}_0)$.

In [4], the free energy expression is obtained in the form (z is the volume fraction of martensite and ϱ the mass density of the material):

$$\Phi(\boldsymbol{\varepsilon}, T, z) = u_0^1 - Ts_0^1 - z\pi_0^f(T) + \frac{1}{2\varrho}(\boldsymbol{\varepsilon} - \boldsymbol{\varepsilon}^{pe})\mathsf{L}(\boldsymbol{\varepsilon} - \boldsymbol{\varepsilon}^{pe}) + c_v\left[(T - T_0) - T\ln\left(\frac{T}{T_0}\right)\right] + \Delta\Phi \tag{4.3}$$

with

$$\begin{aligned} \boldsymbol{\sigma} &= \varrho\frac{\partial\Phi}{\partial\boldsymbol{\varepsilon}} = \mathsf{L}(\boldsymbol{\varepsilon} - \boldsymbol{\varepsilon}^{pe}) = \mathsf{L}\boldsymbol{\varepsilon}^{e}, \\ s &= -\frac{\partial\Phi}{\partial T}, \\ \pi_0^f(T) &= (u_0^1 - u_0^2) - T(s_0^1 - s_0^2) = \Delta u - T\Delta s. \end{aligned} \tag{4.4}$$

π_0^f is the thermodynamic force of the martensitic transformation at stress-free state. u_o^α and s_0^α are the specific energy and entropy of the α phase ($\alpha = 1$ for the austenite and $\alpha = 2$ for the martensite).

The thermodynamical force associated to the phase transition under non-zero stress is:

$$\pi^f = -\frac{\partial\Phi}{\partial z} = \pi_0^f(T) + \gamma\overline{\sigma}/\varrho - \Phi_{it}(1 - 2z). \tag{4.5}$$

The Clausius-Duhem inequality $(\pi^f\,dz \geq 0)$ is chosen to be the criterion of phase transition [4]:

$$\begin{array}{lll} \text{direct transformation} & dz > 0 & \pi^f \geq 0, \\ \text{inverse transformation} & dz < 0 & \pi^f \leq 0, \end{array} \tag{4.6}$$

http://rcin.org.pl

$\pi^f = 0$ represents the absolute equilibrium states of the system. It is unstable if $\Phi_{it} > 0$, what characterizes the martensitic transformations.

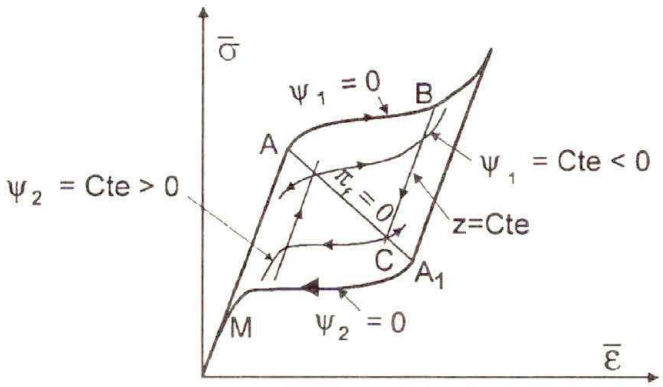

FIG. 19. Description of the external and internal loops in the model of Raniecki et al. [4].

It is then possible to determine the equivalent stress threshold of the martensitic transformation $\bar{\sigma}^{AM}$ (point A in the Fig. 19) and for the reverse transformation $\bar{\sigma}^{MA}$ (point A_1) as:

$$
\begin{aligned}
&\pi^f(\bar{\sigma}^{AM}, z=0, T) = 0 \;\Rightarrow\; \bar{\sigma}^{AM}(T) = \bar{\sigma}^{eq}(z=0) = \varrho\frac{\Phi_{it}(T) - \pi_0^f(T)}{\gamma},\\
&\pi^f(\bar{\sigma}^{MA}, z=1, T) = 0 \;\Rightarrow\; \bar{\sigma}^{MA}(T) = \bar{\sigma}^{eq}(z=1) = \bar{\sigma}^{AM}(T) - 2\varrho\frac{\Phi_{it}(T)}{\gamma}.
\end{aligned}
\tag{4.7}
$$

The instability of the equilibrium yields the conclusion that there exists no thermodynamical relation which could give the equations of the hysteresis loop. Taking a similar framework as in the plasticity approach, the functions Ψ_1 (for the direct transformation) and Ψ_2 (for the reverse one) are assumed to be constant during the phase transition. $\Psi_1 = 0$ and $\Psi_2 = 0$ are the functions which represent the complete martensitic and reverse transformations (they describe the "external loop"). $\Psi_1 = n$ and $\Psi_2 = m$ (m and n are negative constants) represents the internal loops where the transformation is not total.

$$
\begin{aligned}
\Psi_1(\boldsymbol{\sigma}, T, z) &\equiv \pi^f(\boldsymbol{\sigma}, T, z) - k_1(z),\\
\Psi_2(\boldsymbol{\sigma}, T, z) &\equiv -\pi^f(\boldsymbol{\sigma}, T, z) + k_2(z).
\end{aligned}
\tag{4.8}
$$

The functions $k_1(z)$ and $k_2(z)$ are chosen [4] such that the kinetics of the phase transformation are in agreement with the ones proposed by metallurgists [11]:

$$
\begin{aligned}
k_1(z) &= -(A_1 + B_1 z)\ln(1-z) + C_1 z,\\
k_2(z) &= (A_2 - B_2(1-z))\ln z - C_2(1-z)
\end{aligned}
\tag{4.9}
$$

http://rcin.org.pl

with

$$
\begin{aligned}
C_1 &= 2\Phi_{it}(M_s), & C_2 &= 2\Phi_{it}(A_s),\\
a_1A_1 &= \Delta s + \overline{s}_0, & a_2A_2 &= \Delta s - \overline{s}_0,\\
a_1B_1 &= a_2B_2 = 2\overline{s}_0.
\end{aligned}
\tag{4.10}
$$

4.2. Application to a tension-torsion proportional loading test

The behaviour is elastic as long as the equivalent stress does not reach the critical equivalent stress $\overline{\sigma}^{AM}$ $(z = 0)$:

$$
\overline{\sigma}^{AM} = (\sigma_{zz})^{AM}\sqrt{1 + 3\alpha^2}. \tag{4.11}
$$

Then the pseudoelastic behaviour must be simulated. The volume fraction of martensite is increasing from 0 to z_d, which is the z value obtained just before the unloading. The pseudoelastic flow is represented by $\Psi_1 = 0$. It gives:

$$
\pi_0^f + \gamma\overline{\sigma}/\varrho - \Phi_{it}(1 - 2z) = k_1(z). \tag{4.12}
$$

Since during the whole test tensile and torsion stresses are proportional ($\overline{\sigma} = (\sigma_{zz})\sqrt{1 + 3\alpha^2}$ with $\sigma_{z\theta} = \alpha\sigma_{zz}$), it is possible to determine the stress values from the relations

$$
\begin{aligned}
\sigma_{zz} &= \frac{\varrho}{\gamma(1 + 3\alpha^2)}\left[k_1(z) + \Phi_{it}(1 - 2z) - \pi_0^f\right],\\
\sigma_{z\theta} &= \alpha\sigma_{zz}.
\end{aligned}
\tag{4.13}
$$

The corresponding strains follow from (3.6) and (3.11),

$$
\begin{aligned}
\varepsilon_{zz} &= \frac{\sigma_{zz}}{E} + \gamma z,\\
\varepsilon_{z\theta} &= \sigma_{z\theta}\left(\frac{1 + \upsilon}{E} + \frac{3\gamma z}{2\overline{\sigma}}\right).
\end{aligned}
\tag{4.14}
$$

The reverse transformation is represented by the $\Psi_2 = k_2(z_d)$ curve ($k_2(z_d)$ is a negative constant) where z_d is the volumic part of martensite at the end of the loading process. So, during the unloading to the stress σ_1, the stresses are given by

$$
\begin{aligned}
\sigma_{zz} &= \frac{\varrho}{\gamma(1 + 3\alpha^2)}\left[k_2(z) - k_2(z_d) + \Phi_{it}(1 - 2z) - \pi_0^f\right],\\
\sigma_{z\theta} &= \alpha\sigma_{zz}.
\end{aligned}
\tag{4.15}
$$

The corresponding strains are still given by Eq. (4.14).

http://rcin.org.pl

The seven parameters A_1, B_1, C_1, A_2, B_2, C_2 and γ which determine the functions k_1 and the k_2, Φ_{it} and π_0^f are determined from tensile loading tests described in [2] by the following constants.

Δu (Jkg^{-1})	Δs (Jkg^{-1}K^{-1})	$\overline{u}_0$ (Jkg^{-1})	$\overline{s}_0$ (Jkg^{-1}K^{-1})	γ	a_1 (K^{-1})	a_2 (K^{-1})
6 944	23.36	1 495	4.22	0.0416	0.032	0.06

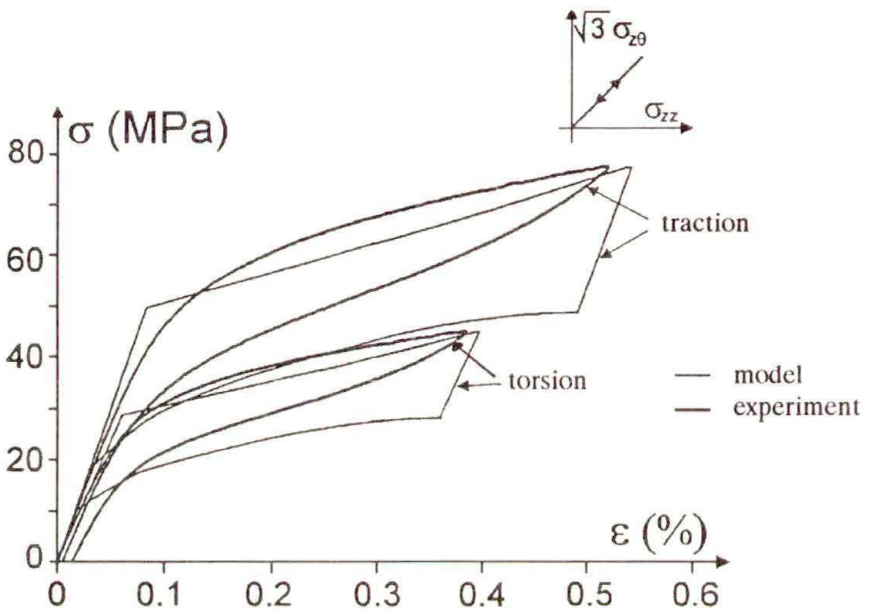

FIG. 20. Experimental and modelled curves concerning the test No. 4.

Modelling of the test No. 4 is presented in the Fig. 20. The form of the theoretical loops are acceptable but some corrections are necessary. The results prove the validity of the 3D model proposed by RANIECKI *et al.* in [4] and the proposed state equations of pseudoelasticity (3.11).

5. Conclusion

Proportional and non-proportional tests have been performed by means of a special experimental device, in order to increase the number of experimental data in the case of complex loading.

Proportional loading tests allows us to verify the normality rule for pseudoelastic strain rate, and hence it enables the experimental verification of the thermodynamical model of pseudoelastic behavior developed by RANIECKI *et al.* in [4]. In the future, other stress-strain curve simulations will be presented.

http://rcin.org.pl

Non-proportional loading tests brought a lot of informations not easy to interprete. It shows the evidence that the pseudoelastic nonlinear behavior depends on the chosen stress path. The main physical features are the creation of new variants (called "secondary" ones) when the stress direction change, or (and) the reorientation of the first variants under the stress.

Only a microstructural observation will allow us to describe the mechanism of martensite plates displacement and creation by the stress path.

For an isothermal pseudoelastic cycling (N_{max} = 35), both proportional and non-proportional training processes are associated with very high efficiency values: this is a very good information for technical applications.

We believe that the analysis of such complex loading processes will help us to understand the S.M.A. pseudoelastic behaviour.

Acknowledgments

We are very grateful to M. G. LAITHIER (CNRS technician) for his precious experimental help.

References

1. L. CONTARDO, *Etude des traitements d'éducation, de la stabilité et de l'origine de l'effet mémoire double sens dans un alliage CuZnAl*, Thèse INSA Lyon, France, No. 88ISAL0048, 1988.
2. C. ROGUEDA, *Modelisation thermodynamique du comportement pseudoélastique des alliages à mémoire de forme*, Thèse Université de Franche-Comté, France, No. 336, 1993.
3. C.M. FRIEND, *The effect of applied stress on the reversible strain in CuZnAl shape memory alloys*, Scripta. Met., 20, 995–998, 1986.
4. B. RANIECKI, C. LEXCELLENT and K. TANAKA, *Thermodynamic models of pseudoelastic behaviour of shape memory alloys*, Arch. Mech., **44**, 3, 261–288, 1992.
5. P. SITTNER, K. HARA and M. TOKUDA, *Pseudoelastic deformation in combined tension and torsion*, [in:] Strength of Materials, OIKAWA *et al.* [Eds.], 319–322, 1994.
6. Z.G. WANG, *Experimental study of mechanical behaviour of Ti Ni shape memory alloys. 2. Multiaxial stress*, Acta Mech. Sinica, [to be published].
7. P. VACHER, *Etude du comportement pseudoélastique d'alliages à mémoire de forme CuZnAl polycristallins*, Thése Université de Franche-Comté, France, No. 215, 1991.
8. R. STALMANS, J.V. HUMBEECK and L. DELAEY, *The two-way memory effect in copper-based shape memory alloy – thermodynamics and mechanisms*, Acta Met. Mater., **40**, 11, 2921–2931, 1992.
9. B.C GOO, *Modélisation micromécanique du comportement thermomécanique d'alliages à mémoire de forme monocristallins et polycristallins*, Thèse Université de Franche-Comté, France, No. 491, 1995.
10. I. MULLER, H. XU, *On the pseudoelastic hysteresis*, Acta. Met. Mat, **39**, 263–271, 1991.
11. D.P. KOISTINEN and R.E. MARBURGER, *A general equation prescribing the extent of the austenite-martensite transformation in pure iron-carbon alloys and plain carbon steels*, Acta. Metall., **7**, 59–70, 1959.

LABORATOIRE DE MÉCANIQUE APPLIQUÉE R. CHALÉAT
UNIVERSITÉ DE FRANCHE-COMTÉ, BESANÇON, FRANCE.

Received February 21, 1996.

http://rcin.org.pl